The LECX experiment onboard the nanoMIRAX satellite

João Braga[(1)], **Otávio S. C. Durão**[(2)]
[(1)] *INPE, Av. dos Astronautas 1758, S. J. Campos, SP, Brazil, +55-12-32087215, joao.braga@inpe.br*
[(2)] *CRON Sistemas e Tecnologias Ltda., Parque Tecnológico UNIVAP, Av. Shishimi Hifumi 2911 anexo 3, S. J. Campos, SP, Brasil, +55-12-997041361, otavio@cronsistec.com.br*

Keywords: *cubesats, X rays, gamma-ray bursts, gravitational waves, detectors*

The nanosat/cubesat revolution has provided new opportunities to develop and launch small (∼1000 cm^3), low-cost (∼US$ 1M) experiments in space in very short timeframes (∼2 years). We present here the development of an astronomical hard X-ray (30-200 keV) experiment, LECX ("Localizador de Explosões Cósmicas de Raios X"), which is the payload of the nanoMIRAX satellite. The mission is designed to detect and localize within a few degrees events like Gamma-Ray Bursts (GRB) and other cosmic explosive phenomena. The experiment uses 4 planar CdZnTe detectors ($10\times10\times2$ cm^3) and a passive shielding system (Pb-Sn-Cu) which determines a $53^\circ\times53^\circ$(FWHM) field-of-view (FoV). The instrumental and aperture background spectra expected during operation in orbit, due the diffuse gamma-ray and particle fields, were calculated using the GEANT4 software package. The experiment sensitivity allows for detection of most known GBRs and the expected detection rate is of up to ∼10 events per year in the experiment's FoV. An algorithm was developed to determine the incoming direction of the X rays during a cosmic burst that occurs in the FoV; the calculations are based on the registered detector counts and the attitude of the satellite. The satellite platform is a 2U CubeSat standardized bus with the LECX experiment, developed by INPE's astrophyscis Division, taking 1 "U" and the satellite service module, built by CRON Sistemas e Tecnologias, taking the other "U". This is the first CubeSat platform developed by the Brazilian private sector. We are currently building the flight model and hope to launch nanoMIRAX in 2023. In the current multimessenger era of astronomy, a constellation or swarm of small spacecraft such as nanoMIRAX can be a very cost-effective way to search for electromagnetic counterparts of gravitational wave events produced by the coalescence of compact objects.

1. Introduction

In order to develop competitive instruments to detect X- and gamma-rays from astrophysical sources, we are usually faced with several limitations which depend on available budget and resources. Non-focusing instruments such as coded-aperture telescopes (see 1 for a recent review) need both large detector areas to maximize source count rates and massive shielding systems to minimize background levels. With the current explosive growth of the nanosat phenomenon based especially on the so-called CubeSat platform, new opportunities for fast-development, low-cost small instruments have appeared.

In principle, X- and gamma-ray astrophysical instruments on such small satellites cannot compete with full-sized instruments operating on conventional large and complex satellite buses. Nevertheless, for very specific science goals, it is possible to

design instruments compatible with cubesat buses that can meet the desired requirements. In this work we describe an instrument developed for a cubesat platform that is capable of not only to detect relatively strong cosmic explosions in the hard X-ray/low energy gamma-ray range but also to determine their position in the sky within a few degrees. The experiment, called "Localizador de Explosões Cósmicas de Raios X" (LECX), will be sensitive enough to detect and localize events like the well-known gamma-ray bursts (GRBs – see 2) in the 30–200 keV energy range. With its $53^\circ \times 53^\circ$ FWHM ("Full Width at Half Maximum") FoV, it is estimated that LECX will detect up to$\sim$ 10 GRBs per year.

In the recently-inaugurated mutimessenger astrophysics era, it is of paramount importance that wide-field space instruments constantly patrol the sky in order to instantly detect electromagnetic (EM) counterparts of gravitational wave (GW) and/or neutrino cosmic bursting events. With the increased sensitivities of ground-based observatories of gravitational waves (e.g. LIGO/VIRGO) and neutrinos (e.g. IceCube), it is expected that the rate of such events will gradually increase over the years. X- and gamma-ray space experiments will then have higher probabilities of contributing to multimessenger detections of such phenomena.

The technology being developed for LECX builds upon what has been developed for the protoMIRAX project [3], a balloon experiment that represents a prototype of the MIRAX (*Monitor e Imageador de Raios X*, in Portuguese) space mission [4, 5].

LECX is in the flight model assembling phase and constitutes the payload of the nanoMIRAX satellite [6], which is based on a 2U-cubesat platform. nanoMIRAX is being developed by the Brazilian private company CRON Sistemas e Tecnologias Ltda. in partnership with INPE (National Institute for Space Research) and strong support from the Brazilian Space Agency (AEB).

2. The detector system and payload module

LECX employs four CdZnTe (CZT) planar detectors in a 2x2 configuration. Each detector is a 10mm x 10mm square with a thickness of 2mm, operating from 30 to 200 keV, described in detail in Braga et al. [3]. The lower limit is imposed by electronics noise and the higher limit is due to detector thickness. CZT room-temperature semiconductor detectors have been extensively used in astronomical X- and γ-ray space instruments due to their very high photoelectrical efficiency up to hundreds of keV and good energy resolution. They are also easy to handle and can be tiled to cover large surfaces. Pixelated CZT detectors can also be built for imaging instruments.

The separation between adjacent detector volumes in the LECX detector array is 3 mm due to the mechanical mounting and the presence of the detectors' ceramic (alumina) substrates. The array is surrounded by a Pb (1.0mm), Sn (1.7mm) and Cu (0.3mm) graded shield box to minimize background and define the instrument FoV. The distance from the detector plane surface to the top of the shielding box is 20mm. In the upper part of the box there is an aperture of 23mm x 23mm that matches the detector plane area below (considering the gaps between the detectors). The area of the aperture is closed with a 0.4mm-thick carbon fibre plate to prevent the entrance of environment light, which induces noise in the detector electronics.

In Figure 1 we see a top view of the detector plane and the shielding walls surrounding the 4 detectors. The detector system is surrounded by a dielectric material (teflon) structure (also shown in the picture) that provides mechanical support and

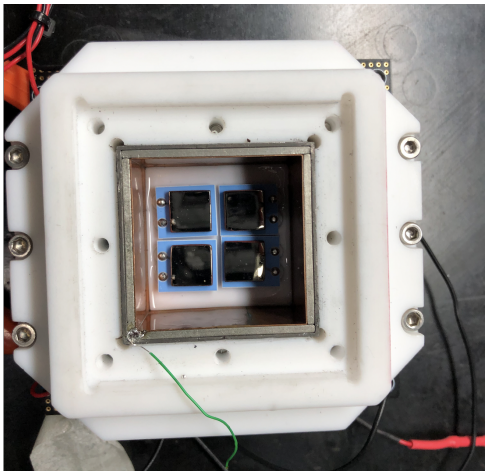

Figure 1: The 4 CZT detectors of LECX placed at the bottom of the shielding box, which is surrounded by the teflon support structure.

housing for batteries and electronic parts. Teflon is widely used in space application due to its suitable mechanical properties. The whole system is mounted on a standard 89mm×89mm cubesat printed-circuit board at the top of the satellite structure (the "top" direction hereafter refers to the instrument axis, i.e. the direction corresponding to the centre of its FoV). The front-end analog electronics for the detectors, which comprises four sets of charge pre-amplifiers and low-noise shaping amplifiers, is mounted on the opposite (bottom) side of the board. This PCB, as well as the other two board of the LECX payload, has multiple interconnected copper layers to provide electrical shielding. At the bottom part of the detector substrates lies the bottom part of the shielding box, so that the two electric leads (the one that polarizes the anode with the reverse bias and the one carrying the charge signal pulse from the cathode) perforate the shielding material, in teflon tubes, in order to reach the PCB underneath. The radiation shielding is also connected to the common ground to contribute to the electrical shielding.

Figure 2 shows two computer-generated pictures of the detector system mounted on a PCB.

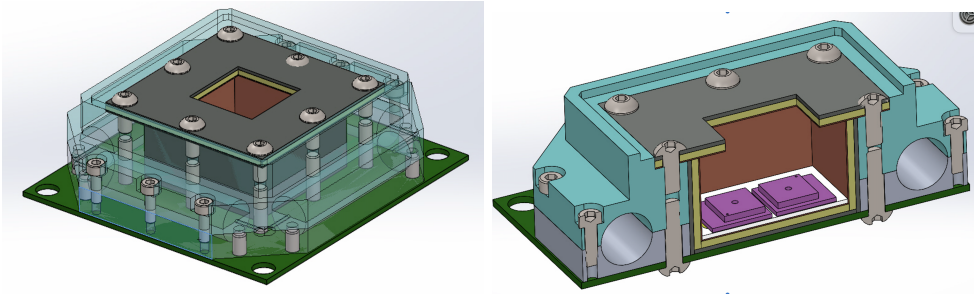

Figure 2: Computer model of the LECX detector system.

The performance of the detector plane has been demonstrated in the protoMIRAX experiment [3]. The reverse bias of -200 V was carefully chosen so as to minimize signal losses due to incomplete charge collection within the CZT material whilst keeping

very low levels of dark current. The long-duration CR1216 Lithium Manganese Dioxide batteries used for the detector power supply are placed close to the detector plane and encapsulated in the teflon structure to avoid current leakage.

A second PCB, mounted underneath the detector board, houses the four Height-Time Converter (HTC) electronics, which linearly converts the heights of the pulses coming from the detectors to a digital high level signal. A third PCB, the experiment on-board-computer or digital board, houses the digital electronics, which is responsible for performing the following tasks: (a) receive signals from the 4 outputs of the TPCB; (b) measure the time duration of the correspondent high level signals and convert them into digital 8-bit words (this is proportional to the deposited energy of each event, divided in 256 channels), (c) flag the individual detector were the event occurred and convert it into a 2-bit word; (d) tag each event with the Universal Time from the satellite on-board computer (OBC), that uses a GPS receiver, with a resolution of 255μs; (e) build the event packages with time, detector ID and energy information (each event will generate a 24-bit word); (f) store data files and send copies to the spacecraft OBC for transmission to ground. The EOBC uses a commercial low power PIC24F32 microcontroller very suitable for this specific application. The power consumption of the LECX electronic system is less than 800 mW.

According to simulations of the radiation level to be measured in orbit the LECX payload will produce $\sim$ 100 bits/s in nominal operation, which will generate $\sim$540 kbits/orbit and $\sim$8.6 Mbits/day of data. Assuming at least one 10-minute ground station passage every orbit, this will require $\sim$900 bits/s telemetry capacity, well below the envisaged capabilities of the satellite.

The three PCBs of the nanoMIRAX payload, which comprise the LECX experiment, fill the first “U” of the satellite and constitute the payload module. The second “U”, the service module, mounted underneath the payload module, houses the subsystems of the satellite platform. Figure 3 shows a photo of the satellite being mounted in the lab, including both the payload module and the service module.

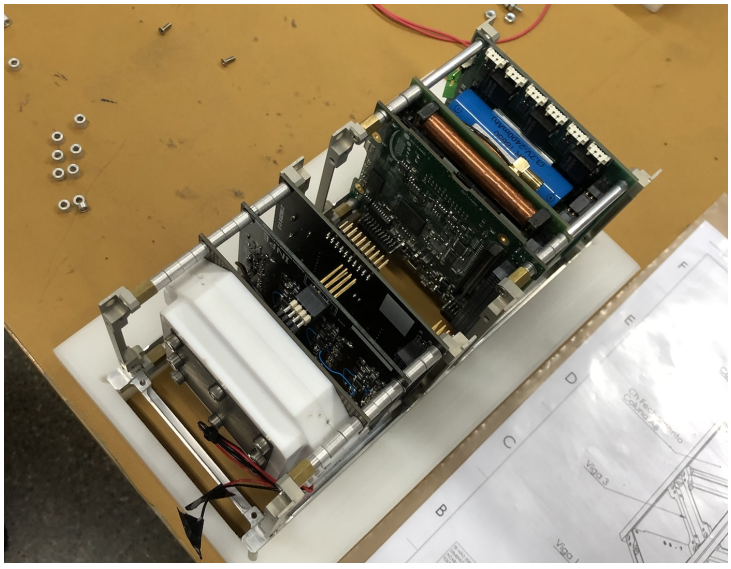

Figure 3: Photo of the nanoMIRAX satellite being mounted on the 2U cubesat structure in the lab.

3. Background and sensitivity

Estimation of the energy spectrum of the background signal and its spatial distribution over the detector plane is crucial for the design of hard X-ray and gamma-ray astronomy telescopes. In the case of an observation of a point source from an orbital space platform (i.e. a satellite), the background consists in the diffuse EM radiation coming through the telescope aperture, emission from other sources in the FOV, and the instrumental background, which arises from interaction of high-energy particles with the detectors and surrounding materials. Therefore, in order to foresee the performance of LECX in orbit and its sensitivity to cosmic explosions, we need to have a good estimate of the background radiation the detectors will measure. We have calculated this using the well-known GEANT4 package [7]. Details of our procedure to calculate the background of an instrument from angle-dependent spectra of photons and particles in space can be found in Castro et al. [8]. Considering a near-equatorial low-Earth orbit (LEO) and a mass model of the LECX experiment, we have obtained the main components of the expected background in orbit, outside the South Atlantic Geomagnetic Anomaly (SAGA). This is shown in Figure 4.

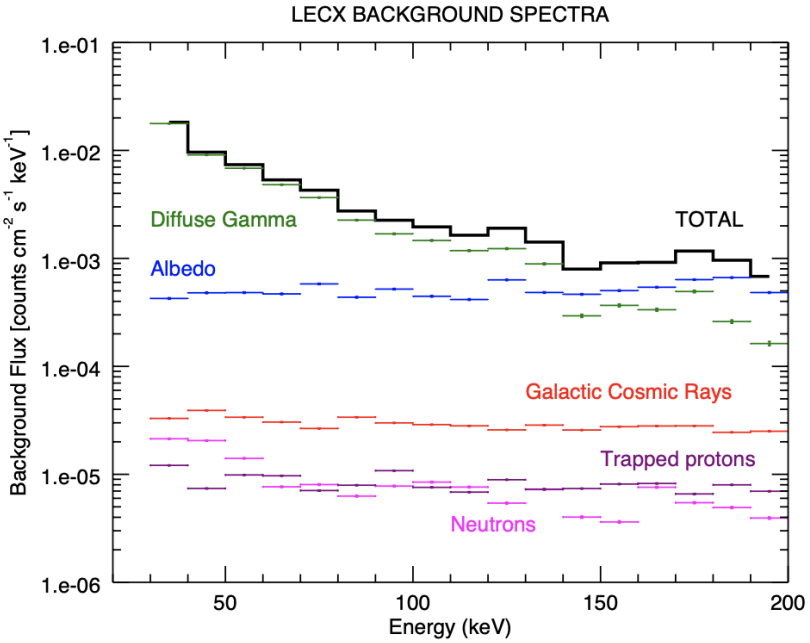

Figure 4: Simulated spectra of the main components of the LECX background in equatorial LEO, considering the 4 detectors as one unit and a spacecraft attitude in which the instrument's axis is pointed to the zenith.

We can see that the main contributions come from the diffuse electromagnetic flux entering the aperture (up to ~ 140 keV) and the albedo radiation coming from the Earth atmosphere (above ~ 150 keV). During the occurrence of a cosmic explosion event, it is reasonable to consider that the Compton-scattered events and fluorescence on the collimator walls will not add significantly to the background that will be present during the event, since the graded-shield walls were specifically designed to minimize these radiations with the help of GEANT4 simulations (see 8).

The sensitivity of LECX can be calculated considering that the number of counts in each detector, for a given integration time and a given energy bin, obey Poisson

statistics. In the case of cosmic explosions observations, what will be measured are sudden increases in the total count rate that will last typically from a fraction of a second to tens of seconds during nominal operation. A trigger mechanism will detect these surges and automatically put the experiment in burst mode, which will end when the low count rates resume. During burst mode, the satellite service module will provide more frequent attitude information data. The electronics is designed so that all events will be time-tagged and stored onboard even if the count rate increases by a factor of ~ 100. All science and spacecraft data will be transmitted to the ground during the ground station passages.

Under nominal operations, the detector system will be measuring background radiation before and after the detected bursting events. We will select the best timescales to get good statistics for the background measurements. Since we may have significant background variations during one orbit, we also have to minimize this integration time to get more accurate values with respect to the background in effect during the occurrence of the event. During the event, we subtract the background counts from the total counts in each selected energy bin to obtain the source spectrum. It is easy to show that the minimum detectable flux, in photons $\mathrm{cm}^{-2}\mathrm{s}^{-1}\mathrm{keV}^{-1}$, for each energy bin ΔE centred on energy E will be

$$F_{\min}(\Delta E) = \frac{N_\sigma}{\epsilon(E)} \sqrt{\frac{B(E)}{A_{\det}\Delta E}\left[\frac{1}{T_B} + \frac{1}{T_S}\right]} \tag{1}$$

where N_σ is the statistical significance (signal-to-noise ratio), $\epsilon(E)$ is the detector efficiency, $B(E)$ is the background in counts $\mathrm{cm}^{-2}\mathrm{s}^{-1}\mathrm{keV}^{-1}$, $A_{\det}$ is the detector geometrical area in cm^2 (in this case $4\,\mathrm{cm}^2$), ΔE the energy bin in keV, T_B the time spent measuring background and T_S in the time spent measuring source+background (both in seconds).

According to the expected count rates, $\sim$5 minutes is a reasonable time to measure background before and after a triggered event, considering a ~ 90-minute orbit. Using then 10 minutes for background integration, we have calculated the on-axis 3-σ sensitivity of LECX for 1, 10, 100 and 1000 seconds. The results are shown on Figure 5.

One can see that LECX is capable of detecting a wide range of typical GRB fluxes even with one-second integrations. For longer-duration GRBs, even somewhat weak events could be detected. The Crab spectrum [9] is shown in the figure just for comparison purposes, since the Crab it is a strong standard candle in these energies. LECX will not be able to detect the Crab since it would require pointing and very long stabilized observations, capabilities that the nanoMIRAX satellite will not have.

4. The localization algorithm

With the four CZT detectors placed inside the passive shielding box, the FoV of the detector system is a square region of the sky of $53^\circ \times 53^\circ$ FWHM ($\approx$ 7% of the sky) and $90^\circ \times 90^\circ$ FWZI ("Full Width at Zero Intensity"). In this section we describe the original algorithm we have devised to determine the celestial coordinates of strong cosmic explosions inside this FoV based on the intensities measured in each detector during the event.

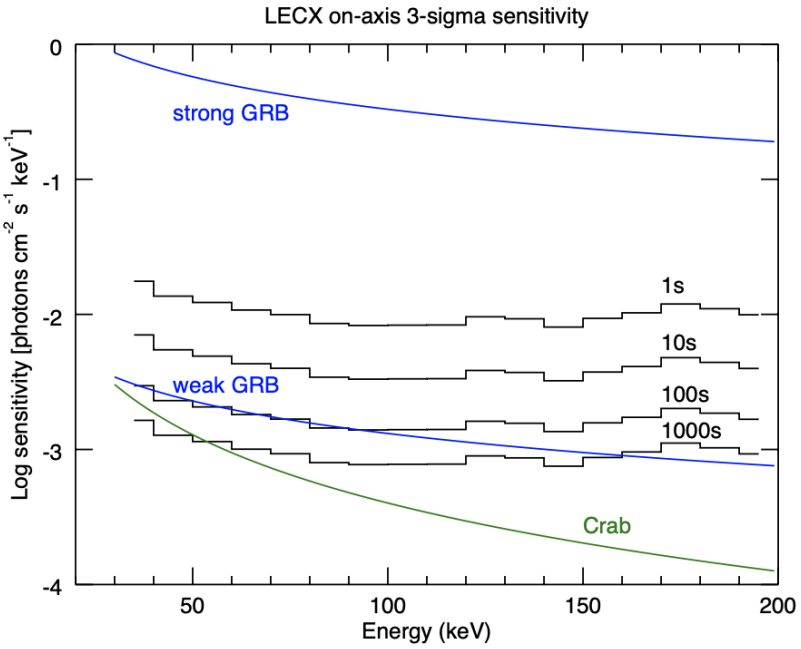

Figure 5: On-axis 3-σ sensitivity (minimum detectable flux) of LECX for different on-source integration times, considering 10 minutes for background integration. Strong and weak GRB spectra are shown in blue and the Crab spectra is shown in green for comparison.

In standard collimated high-energy detector systems, the fluxes of astrophysical sources are determined by subtracting a background level, measured separately, from the amount of radiation measured when the source is in the collimator FoV. For pixelated detector planes, one can use a coded mask in the aperture to obtain an image of the source field within the FoV (see, e.g. 1). In the LECX cubesat experiment described here, we have only 4 pixels (the four planar detectors) and a limited sensitivity due to the fact that the total area is only 4 cm^2. Since we are interested in detecting strong, short-duration point-source cosmic explosions one at a time, a coded mask placed in the experiment's aperture will not be adequate to use due to two main reasons: (a) the results to be obtained are not images of source fields, but only measured fluxes of short-duration ($\sim$ seconds) point sources; and (b) the advantage of coded-mask systems in measuring source and background simultaneously are not important here, since we will have plenty of time to measure the background anyway, and in the same region of the sky.

During the detection of a radiation burst coming from a single direction (representing a cosmic explosion), the x and y extensions (with respect to the square shielding box and detector orientations) of the wall shadows on the detector plane is a function of the azimuth and zenith angles of the incoming photons. Since the number of source counts in each detector is proportional to the illuminated area, we can determine the source position in the sky by measuring the counts in each detector when the count rates suddenly increase during the occurrence of such an event in the FoV.

To explain the method, let us first define a coordinate system with axes x and y along the detector sides for a given detector plane orientation in which (looking from above the detector plane) "North" is to the upper direction (y axis) and "East" is to

the right (x axis). The relevant units of distance are the detector side s (10mm in this case) and the height of the shielding walls above the detector surface, H (20mm). Starting from the upper left corner, let us call the detectors D_{11}, D_{12}, D_{21} and D_{22}, going clockwise.

If a cosmic explosion occurs in the FoV, let us define its direction by the "zenith angle" z with respect to the z axis, and the Azimuth angle A, defined in the $x-y$ plane, starting at the y axis (the "North" direction) and increasing clockwise. In this case, the x and y extensions of the shadows of the shielding walls over the detector plane will clearly be

$$L_x = H \tan z \cos A \quad ; \quad L_y = \tan z \sin A \tag{2}$$

Now, starting from the upper left corner, let us call the detector illuminated areas A_{11}, A_{12}, A_{22} and A_{21}, following the detector labels. If the explosive event happens in the "SouthEast" quadrant, then

$$\begin{aligned} A_{11} &= s^2 \qquad ; \quad A_{12} = s(s - L_x) \\ A_{21} &= s(s - L_y) \qquad ; \quad A_{22} = (s - L_x)(s - L_y) \end{aligned} \tag{3}$$

since D_{11} will be fully illuminated, D_{12} and D_{21} will be shadowed by one wall each and D_{22} will have shadows from two walls.

In the general case, the algorithm first identifies the quadrant where the incoming direction lies by finding the detector with the most counts. Then it flags the other detectors in a decreasing order of counts. We then solve equations in the form of equations 3 (depending on the quadrant) for L_x and L_y, and finally use equations 2 to find A and z. The algorithm reproduces the incoming angles exactly when no statistical fluctuations are present.

For large zenith angles of incidence ($z > \arctan(s/H)$ in the orthogonal directions and up to $z > \arctan(\sqrt{2}s/H$ in the diagonal directions), the radiation coming from the source will miss one line of detectors entirely. In those cases, the algorithm can only determine ranges of A and z due to the lack of information from the four detector count numbers, which prevents us from calculating count ratios between detectors. Even in those cases, it is noteworthy that we can still get some localization despite using a very simple experimental setup. In particular, if the EM burst is coincident with a gravitational wave event, any independent localization may prove to be useful since the GW laser-interferometric detectors have poor localization capabilities. With the FoV of LECX, it is expected that the mission will detect up to ~ 10 cosmic explosions per year.

5. Simulation of cosmic explosions

In order to predict the performance of LECX for observations of GRBs and related phenomena, we have carried out a series of Monte Carlo simulations taking into account typical GRB spectra and the predicted LECX background. The details of these simulations can be found in [10].

GRBs are brief flashes of γ-rays with spectral energy distributions that peak around hundreds of keV and are expected to be detectable at a rate of ~ 1 event per day in the entire sky with the currently available instrumentation [11]. They represent the most energetic explosions in the Universe and can release up to 10^{54} ergs in a few seconds. GRBs follow a bimodal distribution in which most of the bursts last longer than ~ 2

seconds, clustering around tens of seconds, and about $1/3$ of them are shorter, clustering around 400 ms. The former are believed to be produced by the core collapse of massive, high-rotation stars, whereas the latter are best explained by the coalescence of neutron stars in a binary system. These short bursts are additionally interesting because they are expected to emit copious amounts of energy in the form of gravitational waves, as was dramatically demonstrated by the GW 170817 event (e.g. 12). As the current gravitational wave detectors (LIGO and VIRGO) are upgrading their sensitivities and new ones (KAGRA, LIGO-India) are about to start operating, it is expected that the rate of GW burst discoveries will significantly increase over the next years. It is extremely important that those detections are accompanied simultaneously by X- and γ-ray observations, since the GW instruments lack precise angular localization and the EM signals are complementary with respect to the characterization of the source. In a sense, we "see" the event through EM signals and "hear" it through the GW signal.

Short GRBs (SGRBs) usually have harder spectra and are less energetic than long GRBs [13]. However, the fluxes detected at Earth vary by several orders of magnitude depending on the GRB distance. The time-integrated fluxes (fluences) for all GRBs range approximately from 10^{-8} to 10^{-4} erg cm^{-2}. The observed photon spectra also show significant diversity and can usually be fit with the so-called Band model, a broken power-law with a smooth junction [14]. In any event, since we are interested in order-of-magnitude values for the simulations, we can approximately consider that a typical GRB photon spectrum measured at Earth is $F = AE^{-1}$, where A varies from 0.25 (weakest GRBs) to 200 (strongest GRBs), E is measured in keV and F is given in photons cm^{-2}s^{-1}keV^{-1}. This corresponds to a flat νF_ν spectrum. Figure 5 shows the limiting cases of these spectra.

In the simulations, we have considered the LECX instrument in a near-equatorial LEO and an incident flux coming from a GRB in a given direction. If on-axis, a very strong GRB would produce $\sim$1,900 counts in 1 s in the 30-200 keV energy range, whereas a very weak GRB would produce $\sim$2 counts. The background rate calculated using the GEANT4 simulations is $\sim$2.5 counts/s.

Using these numbers, we can simulate the signal-to-noise ratio (SNR) and the localization accuracy that we could achieve in a GRB detection with LECX. For the simulations reported here, we first calculate the illuminated areas on the four detectors, defined by the direction in the sky from which the photons are coming. In the real observations, this will depend not only on the azimuth and elevation with respect to the experiment reference frame but also on the satellite attitude given by the spacecraft's attitude control system. By combining the two coordinate systems, we then determine the celestial coordinates (e.g. right ascension and declination) of the event in the sky.

Once the illuminated areas are defined, we simulate random source counts at the level of the known sources in each detector using a Poisson distribution. These numbers scale with the illuminated fraction of the detector areas. The source counts are calculated convolving the source spectra with the response function of the instrument, which is given by the ratio of the effective area to the geometrical area of the detectors as a function of energy. In this case this will be essentially the photoelectric efficiency of the CZT detectors, since in these detectors the photoelectric effect is highly favoured with respect to Compton scatterings up to several hundred keV [15]. The background counts added to that are also Poissonian distributed and are given by the values provided by the GEANT4 simulations.

As a first example, we simulated a strong GRB occurring at $A = 20^\circ$ and $z = 5^\circ$.

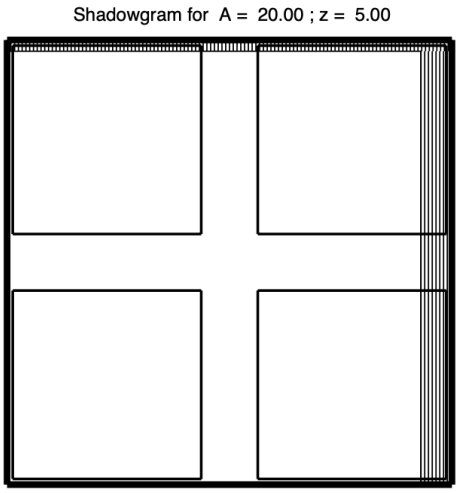

Figure 6: The detector shadow geometry for a strong GRB simulation. The simulated position in the sky is $A = 20°$ and $z = 5°$.

Figure 6 shows the shadow position at the detector plane. In this case we get a theoretical (Poissonian) SNR of ~ 37. After repeating the simulation 100 times to determine the dispersion on the parameters, we get $A = 8.94 \pm 24°$ and $z = 6.13 \pm 2°$. The values of the dispersions do not vary significantly for more than ~ 5 repetitions of the simulations, so these 1-σ dispersion values are very robust. The SNR of the detection is in close agreement with the Poissonian theoretical value. Figure 7 shows the 1-σ sky localization region for the GRB.

In a second example, we repeated the azimuth angle $(20°)$ but simulated a burst coming at $z = 20°$. The shadowgram is shown in Figure 8 and the localization box in 9.

It is noteworthy that, even though we get less counts due to the fact a larger area is shadowed (which is reflected by a smaller SNR of 19) , the algorithm gives a better determination of the localization of the source in the sky. This is due to the fact that the source is farther away from the instrument axis, which provides a higher contrast among the illuminated areas in the detectors.

A third example shows an explosion that happens outside the FWHM FoV, so that the wall shadows miss completely one line of detectors (see Figures 10 and 11). In this case the "zenith" angle is 40°.

Since two detectors do not register counts, the algorithm can only determine ranges of possible angles for the source position in the sky due to the lack of information from the four detector count numbers, which prevents us from calculating count ratios between detectors. Even in those cases, it is noteworthy that we can still get some localization despite using a very simple experimental setup.

Since the satellite attitude determination precision is of $\sim 1°$ and we do not expect the spacecraft to rotate by more than 1° in 10 s, the conversion of instrument to sky coordinates will have an error of $\lesssim 1°$, which will be a small fraction of the overall localization power for most detected GRBs.

These simulations demonstrate that LECX is able to detect cosmic explosions and determine their positions in the sky with enough accuracy to contribute to the search for EM counterparts of GW burst events detected by the new generation of GW laser-interferometric observatories.

Based on current estimates of GRB occurrence rates and LECX's sensitivity, we

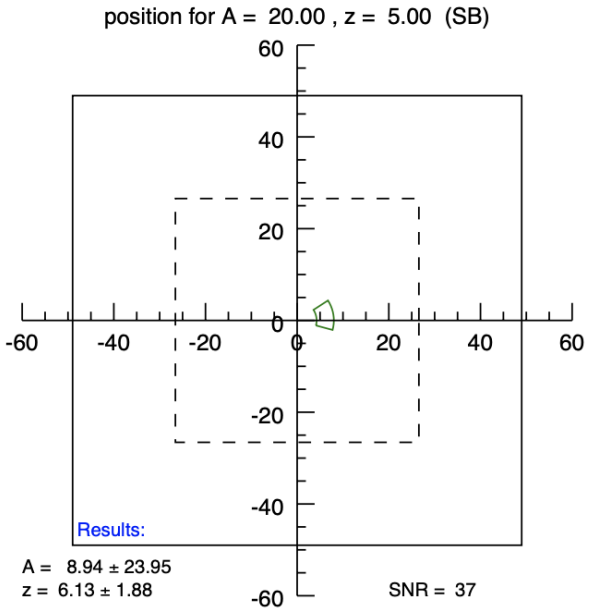

Figure 7: A simulated localization for a strong GRB. The green box gives the 1-sigma localization (in degrees) provided by the localization algorithm developed in this work. A and z are the polar angles (in degrees) in this plot, and the x and y coordinates are in degrees. The dashed square is the FWHM FoV (7% of the sky) and the solid square is the total FoV.

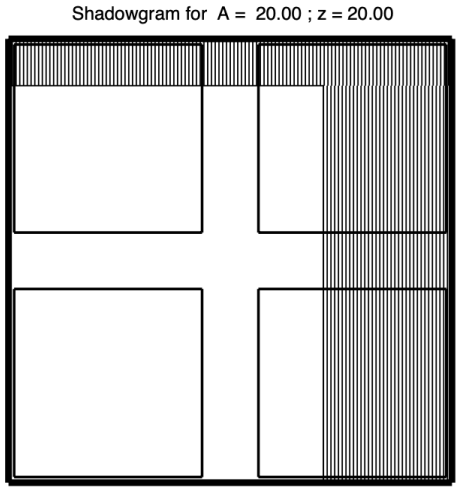

Figure 8: The detector shadow geometry for a strong GRB simulation. The simulated position in the sky is $A = 20°$ and $z = 20°$.

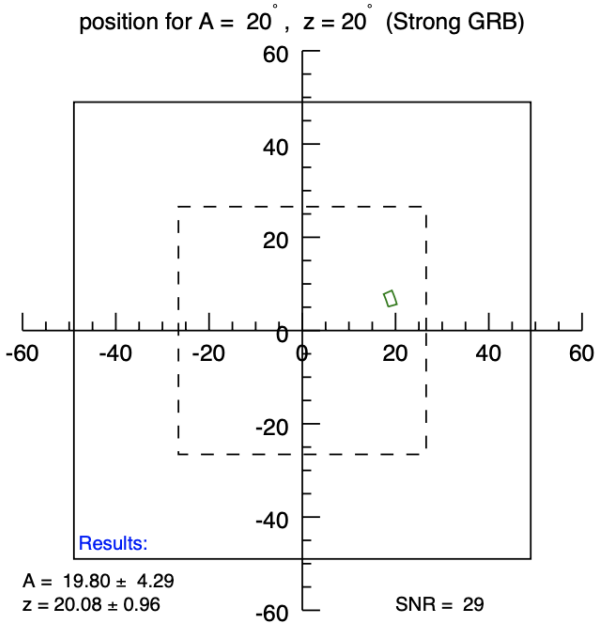

Figure 9: A simulated localization for a strong GRB. The green box gives the 1-sigma localization (in degrees) provided by the localization algorithm developed in this work. A and z are the polar angles (in degrees) in this plot, and the x and y coordinates are in degrees. The dashed square is the FWHM FoV (7% of the sky) and the solid square is the total FoV.

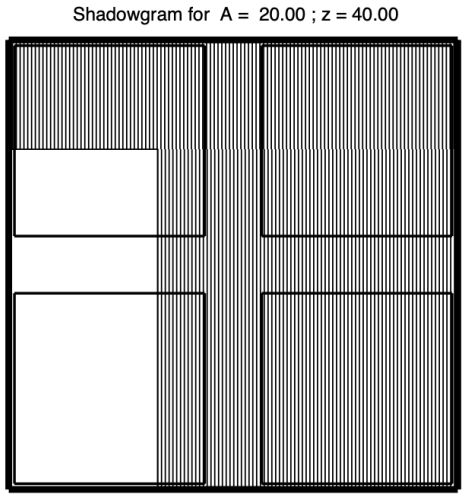

Figure 10: The detector shadow geometry for a strong GRB simulation. The simulated position in the sky is $A = 20°$ and $z = 40°$.

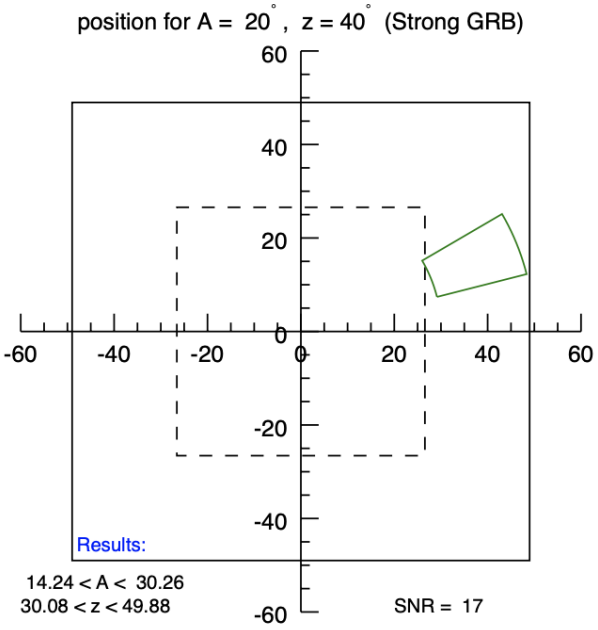

Figure 11: A simulated localization for a strong GRB. The green box gives the 1-sigma localization (in degrees) provided by the localization algorithm developed in this work. A and z are the polar angles (in degrees) in this plot, and the x and y coordinates are in degrees. The dashed square is the FWHM FoV (7% of the sky) and the solid square is the total FoV.

can estimate the rate at which we will be able to detect these events in our FOV. See [10] for details. Our best estimates is that, since our FWHM FOV covers 7% of the sky, this would allow us to detect ~ 10 events per year or ~ 1 event every 36 days.

It is important to stress that the GRB rate in the Universe is still subject to considerable debate, and the fact that the only localized neutron-star/neutron star coalescence event localized so far (GW170817 – 16) was also seen in gamma rays [17] seems to point towards more frequent multi-messenger observations of these events than previously thought.

6. Conclusion

LECX is a small high-energy astrophysics space experiment that is capable of contributing to the detection and localization of cosmic explosions that are characterized by intense emission of hard X-rays and low-energy γ-rays. The nanosat/cubesat revolution has opened new opportunities for the development of scientific space missions in the "smaller, faster and cheaper" paradigm. With creative ideas, it is possible to contribute to science with low budgets and limited resources. The experiment described here is an example of a cubesat mission that is capable of doing competitive and important science by detecting and localizing cosmic explosions in the gravitational wave era of astronomy. This is accomplished by a new algorithm that uses the shadowing of shielding walls over the detector plane to reconstruct the incoming directions of photons coming from a bright and short-lived cosmic point source.

Simulations described here show that LECX can detect most GRBs and locate them within a few degrees in the sky at a rate of $\sim$ 10 per year. With a constellation of satellites of this kind, it would be possible to increase this rate significantly and

provide a low-cost, fast-development network of electromagnetic localizers of gravitational wave events that could complement the observations made by the ground-based gravitational wave observatories.

LECX is currently in the phase of assembling its flight model. We are analyzing launch opportunities and we expect to have the satellite launched by the end of 2023.

In Table 1 we present the baseline numbers of the LECX/nanoMIRAX mission.

Table 1: nanoMIRAX/LECX baseline parameters

LECX payload
Detector type: CdZnTe (CZT)
Dimensions: 10 mm $\times$ 10 mm $\times$ 2 mm (thickness)
Number of detectors: 4 (2×2)
Gap between detectors: 3 mm
Energy Range: $30 - 200$ keV
Geometrical area: 4 cm^2
Effective area: 3.9 cm^2@ 80 keV, 2.1 cm^2@ 150 keV
Energy resolution: 11% @ 60 keV
Time resolution: 255 μs
Expected nominal counting rate: 2.5 counts/s
(up to $\sim$ 100 counts/s in burst mode)
Shielding: Pb (external – 1.0 mm)
Sn (middle – 1.7 mm)
Cu (internal – 0.3 mm)
configuration: box around detectors with
23mm $\times$ 23mm aperture on top, 20mm height
Field of view: $53^\circ \times 53^\circ$ (FWHM); $90^\circ \times 90^\circ$ (FWZI)
Sensitivity: 10^{-2}photons cm^{-2}s^{-1}keV^{-1} for 1 s @ 100 keV
Cosmic Explosion (CE) Location Accuracy: a few degrees
(depending on position and intensity)
Expected CE detection rate: $\sim$ 10 per year
Science data creation rate: 100 bits/s
Payload mass: $\sim$ 600 g
nanoMIRAX satellite
Structure: 2U cubesat frame
Satellite dimensions: 20 cm $\times$ 10 cm $\times$ 10 cm
Total mass: $\sim$ 2.6 kg (including payload)
Power: 2.2 W total, 800 mW delivered to payload
Stabilization: $\lesssim 0.^\circ 1$/s
Attitude knowledge: $\sim 1^\circ$
Communications: Telemetry (download): UHF, 482–486 MHz
Command upload: VHF, 130–160 MHz
Both at 1200–9600 bit/s
Orbit: TBD (possibly polar LEO)
Ground stations: 2 in Brazil (Santa Maria and Natal

Acknowledgments

We thank FAPESP and AEB for support.

References

[1] J. Braga, Coded Aperture Imaging in High-energy Astrophysics, Publications of the Astronomical Society of the Pacific: Invited Review Article 132 (2020) 012001.
[2] B. Zhang, The Physics of Gamma-Ray Bursts, Cambridge University Press, 2018.
[3] J. Braga, F. D'Amico, M. A. C. Avila, A. V. Penacchioni, J. Rodrigo Sacahui, V. A. de Santiago, F. Mattiello-Francisco, C. Strauss, M. A. A. Fialho, The protoMIRAX hard X-ray imaging balloon experiment, Astronomy and Astrophysics 580 (2015) A108.
[4] J. Braga, MIRAX Mission Overview and Status, in: F. D'Amico, J. Braga, R. E. Rothschild (Eds.), The Transient Milky Way: A Perspective for MIRAX, volume 840 of *American Institute of Physics Conference Series*, pp. 3–7.
[5] J. Braga, R. Rothschild, J. Heise, R. Staubert, R. Remillard, F. D'Amico, F. Jablonski, W. Heindl, J. Matteson, E. Kuulkers, J. Wilms, E. Kendziorra, MIRAX: a Brazilian X-ray astronomy satellite mission, Advances in Space Research 34 (2004) 2657–2661.
[6] O. S. C. Durão, J. Braga, V. R. Schad, M. B. Silva Neto, M. Esper, G. Rigobello, C. B. Ribeiro, CRON-1 – The First Brazilian Private Cubesat, Proceedings of the 2019 Small Satellite Conference (2019) 9.
[7] S. Agostinelli, J. Allison, K. Amako, J. Apostolakis, H. Araujo, P. Arce, M. Asai, D. Axen, S. Banerjee, G. Barrand, F. Behner, L. Bellagamba, J. Boudreau, L. Broglia, A. Brunengo, H. Burkhardt, S. Chauvie, J. Chuma, R. Chytracek, G. Cooperman, G. Cosmo, P. Degtyarenko, A. Dell'Acqua, G. Depaola, D. Dietrich, R. Enami, A. Feliciello, C. Ferguson, H. Fesefeldt, G. Folger, F. Foppiano, A. Forti, S. Garelli, S. Giani, R. Giannitrapani, D. Gibin, J. G. Cadenas, I. González, G. G. Abril, G. Greeniaus, W. Greiner, V. Grichine, A. Grossheim, S. Guatelli, P. Gumplinger, R. Hamatsu, K. Hashimoto, H. Hasui, A. Heikkinen, A. Howard, V. Ivanchenko, A. Johnson, F. Jones, J. Kallenbach, N. Kanaya, M. Kawabata, Y. Kawabata, M. Kawaguti, S. Kelner, P. Kent, A. Kimura, T. Kodama, R. Kokoulin, M. Kossov, H. Kurashige, E. Lamanna, T. Lampén, V. Lara, V. Lefebure, F. Lei, M. Liendl, W. Lockman, F. Longo, S. Magni, M. Maire, E. Medernach, K. Minamimoto, P. M. de Freitas, Y. Morita, K. Murakami, M. Nagamatu, R. Nartallo, P. Nieminen, T. Nishimura, K. Ohtsubo, M. Okamura, S. O'Neale, Y. Oohata, K. Paech, J. Perl, A. Pfeiffer, M. Pia, F. Ranjard, A. Rybin, S. Sadilov, E. D. Salvo, G. Santin, T. Sasaki, N. Savvas, Y. Sawada, S. Scherer, S. Sei, V. Sirotenko, D. Smith, N. Starkov, H. Stoecker, J. Sulkimo, M. Takahata, S. Tanaka, E. Tcherniaev, E. S. Tehrani, M. Tropeano, P. Truscott, H. Uno, L. Urban, P. Urban, M. Verderi, A. Walkden, W. Wander, H. Weber, J. Wellisch, T. Wenaus, D. Williams, D. Wright, T. Yamada, H. Yoshida, D. Zschiesche, Geant4 - a simulation toolkit, Nuclear Instruments and Methods in Physics Research Section A: Accelerators, Spectrometers, Detectors and Associated Equipment 506 (2003) 250 – 303.
[8] M. Castro, J. Braga, A. Penacchioni, F. D'Amico, R. Sacahui, Background and imaging simulations for the hard X-ray camera of the MIRAX mission, Monthly Notices of the Royal Astronomical Society 459 (2016) 3917–3928.
[9] P. Wallyn, J. C. Ling, W. A. Mahoney, W. A. Wheaton, P. Durouchoux, BATSE Search for the ~540 keV Feature in the Crab Spectrum Observed by Granat-SIGMA, The Astrophysical Journal 559 (2001) 342–345.
[10] J. Braga, O. S. C. Durão, M. Castro, F. D'Amico, P. E. Stecchini, S. Amirábile, F. Gonzalez Blanco, C. Strauss, W. Silva, V. R. Schad, L. A. Reitano, LECX: a cubesat experiment to detect and localize cosmic explosions in hard X-rays, Monthly Notices of the Royal Astronomical Society 493 (2020) 4852–4860.
[11] D. Williams, J. A. Clark, A. R. Williamson, I. S. Heng, Constraints on Short, Hard Gamma-Ray Burst Beaming Angles from Gravitational Wave Observations, The Astrophysical Journal Letters 858 (2018) 79.
[12] J. Granot, D. Guetta, R. Gill, Lessons from the Short GRB 170817A: The First Gravitational-wave Detection of a Binary Neutron Star Merger, The Astrophysical Journal Letters 850 (2017) L24.
[13] E. Berger, Short-Duration Gamma-Ray Bursts, Annual Review of Astronomy and Astrophysics 52 (2014) 43–105.
[14] D. Band, J. Matteson, L. Ford, B. Schaefer, D. Palmer, B. Teegarden, T. Cline, M. Briggs, W. Paciesas, G. Pendleton, G. Fishman, C. Kouveliotou, C. Meegan, R. Wilson, P. Lestrade, BATSE

Observations of Gamma-Ray Burst Spectra. I. Spectral Diversity, The Astrophysical Journal 413 (1993) 281.

[15] S. Del Sordo, L. Abbene, E. Caroli, A. M. Mancini, A. Zappettini, P. Ubertini, Progress in the Development of CdTe and CdZnTe Semiconductor Radiation Detectors for Astrophysical and Medical Applications, Sensors 9 (2009) 3491–3526.

[16] B. P. Abbott, R. Abbott, T. D. Abbott, F. Acernese, K. Ackley, C. Adams, T. Adams, P. Addesso, R. X. Adhikari, V. B. Adya, C. Affeldt, Multi-messenger Observations of a Binary Neutron Star Merger, The Astrophysical Journal Letters 848 (2017) L12.

[17] B. P. Abbott, R. Abbott, T. D. Abbott, F. Acernese, K. Ackley, C. Adams, T. Adams, P. Addesso, R. X. Adhikari, V. B. Adya, C. Affeldt, Gravitational Waves and Gamma-Rays from a Binary Neutron Star Merger: GW170817 and GRB 170817A, The Astrophysical Journal Letters 848 (2017) L13.